

HANDBOOK OF X-RAY PHOTOELECTRON SPECTROSCOPY

A Reference Book of Standard Data
For Use In
X-Ray Photoelectron Spectroscopy

*© Copyright 1979
By
Perkin-Elmer Corp.*

By
C.D. Wagner
W.M. Riggs
L.E. Davis
J.F. Moulder
G.E. Muilenberg (Editor)

Published By
(Perkin-Elmer Corporation, 1979)
Physical Electronics Division
6509 Flying Cloud Drive
Eden Prairie, Minnesota 55344

© Copyright 1979

By

Perkin-Elmer Corporation

Physical Electronics Division

Printed in U.S.A.

All rights reserved

This book, or parts thereof, may not
be reproduced in any form without
permission of the publishers.

Preface

X-Ray Photoelectron Spectroscopy (XPS), more popularly known as Electron Spectroscopy for Chemical Analysis (ESCA), is now a widely-used analytical technique for investigating the chemical composition of solid surfaces. Much has already been written concerning the principles of the technique and the diverse range of applications for which it has been used. Until now, however, a concise reference work has not been available to the ESCA practitioner. Thus, we felt it desirable to assemble in a single, compact volume much of the information required by those persons using ESCA on a routine basis.

Some users of this Handbook will recognize strong similarities between it and the *Handbook of Auger Electron Spectroscopy*, also published by Physical Electronics. This is natural since there are many similarities between ESCA and Auger spectroscopy and much was learned from publishing two editions of the Auger Handbook. As in the previous Handbook, we include broad scan spectra of most of the elements, as well as spectra from a number of oxides to indicate the differences between elemental states and ionic

forms. Also included is a lengthy discussion of the ESCA technique and its use.

In many ways, ESCA is more complex than Auger spectroscopy. Both photoelectron lines and Auger lines are found in the spectra and a variety of satellite and other lines must be understood. In addition, more detailed chemical information can be obtained if exact line positions can be determined. For these reasons, the *Handbook of X-Ray Photoelectron Spectroscopy* contains much precise spectroscopic energy information, including amplified Auger spectra and amplified strong line photoelectron spectra.

This Handbook is meant to serve as a guide and reference work for the long-time ESCA practitioner as well as the newcomer to the ESCA field. We sincerely hope it serves this purpose and plays a useful role in the practice of x-ray photoelectron spectroscopy.

PERKIN-ELMER
Physical Electronics Division
December, 1978

Contents

I. X-ray Photoelectron Spectroscopy	1
1. Introduction	3
2. Principles of the Technique	4
3. Preparing and Mounting Samples	6
A. Removal of Volatile Material	6
B. Removal of Non-volatile Organic Contaminants	6
C. Surface Etching	6
D. Abrasion	7
E. Fracture and Scraping	7
F. Grinding to Powder	7
G. Mounting Powders for Analysis	7
H. Considerations of Mounting Angle	8
4. Experimental Procedure	8
A. Experimental Technique for Obtaining Spectra	8
B. Instrument Calibration	10
C. Programming Scans for An Unknown Sample	10
(1) Survey Scans	
(2) Detail Scans	
5. Data Interpretation	12
A. The Nature of the Spectrum	12
(1) General Features	
(2) Kinds of Lines	
B. Line Identification	16
C. Chemical State Identification	17
(1) Determination of Static Charge on Insulators	
(2) Photoelectron Line Chemical Shifts and Separations	
(3) Auger Line Chemical Shifts and the Auger Parameter	
(4) Satellite Lines and Peak Shapes	
D. Quantitative Analysis	21
E. Determination of Element Location	23
6. How To Use This Handbook	27
II. Standard ESCA Spectra of the Elements and Line Energy Information	29
1. Tables of Auger Parameter Data	168
2. References for Line Energy Information	174
III. Appendix	179
Table 1. Line Positions from Mg X-rays (by element)	182
Table 2. Line Positions from Al X-rays (by element)	184
Table 3. Line Positions from Mg X-rays (numerical order)	186
Table 4. Line Positions from Al X-rays (numerical order)	187
Table 5. Atomic Sensitivity Factors	188
Table 6. Periodic Table of the Elements	189
Table 7. Alphabetical Index of the Spectra	190

I. X-RAY PHOTOELECTRON SPECTROSCOPY

1. Introduction

Surface analysis by ESCA involves irradiation of the solid in vacuo with monoenergetic soft x-rays and sorting the emitted electrons by energy. The spectrum obtained is a plot of the number of emitted electrons per energy interval versus their kinetic energy. Each element has a unique elemental spectrum, and the spectral peaks from a mixture are approximately the sum of the elemental peaks from the individual constituents. Since the mean free path of the electrons is very small, the electrons which are detected originate from only the top few atomic layers. Quantitative data can be obtained from the peak heights or areas and identification of chemical states often can be made from the exact positions and separations of the peaks, as well as from certain spectral contours.

This Handbook is designed to furnish the user with much of the information necessary to use ESCA for diverse types of surface analysis. Information is provided on methods of sample preparation, data gathering, identifying elements present, identifying the chemical states of surface constituents, obtaining quantitative information on the elements present, and determining elemental distribution by depth and by phase.

Survey spectra, strong line spectra, and Auger group spectra (x-ray excited) for most of the elements and some of their compounds are included. Plots and tables of spectroscopic energy data that will aid in the identification of chemical states are also included with the spectral information.

2. Principles of the Technique

Surface analysis by x-ray photoelectron spectroscopy (XPS), more commonly known as electron spectroscopy for chemical analysis (ESCA), is accomplished by irradiating a sample with monoenergetic soft x-rays and energy analyzing the electrons emitted. MgK α x-rays (1253.6 eV) or AlK α x-rays (1486.6 eV) are ordinarily used. These photons have limited penetrating power in a solid, of the order of 1-10 micrometers. They interact with atoms in this surface region by the photoelectric effect, causing electrons to be emitted. The emitted electrons have kinetic energies given by:

$$KE = h\nu - BE - \phi_s \quad (1)$$

where $h\nu$ is the energy of the photon, BE is the binding energy of the atomic orbital from which the electron originates, and ϕ_s is the spectrometer work function.

The binding energy may be regarded as an ionization energy of the atom for the particular shell involved. Since there is a variety of possible ions from each type of atom, there is a corresponding variety of kinetic energies of the emitted electrons. Moreover, there is a different probability, or cross-section, for each process. The variety of ionization processes for iron and uranium are shown schematically in Figure 1. The Fermi level corresponds to zero binding energy (by definition), and the depth beneath the Fermi level in the Figure indicates the relative energy of the ion remaining after electron emission, or the binding energy of the electron. The lengths of the lines indicate the relative probabilities of the various ionization processes. The p, d, and f levels become split upon ionization, leading to vacancies in the $p_{1/2}$, $p_{3/2}$, $d_{3/2}$, $d_{5/2}$, $f_{5/2}$, and $f_{7/2}$ in the ratio 1:2 for p levels, 2:3 for d levels, and 3:4 for f levels.

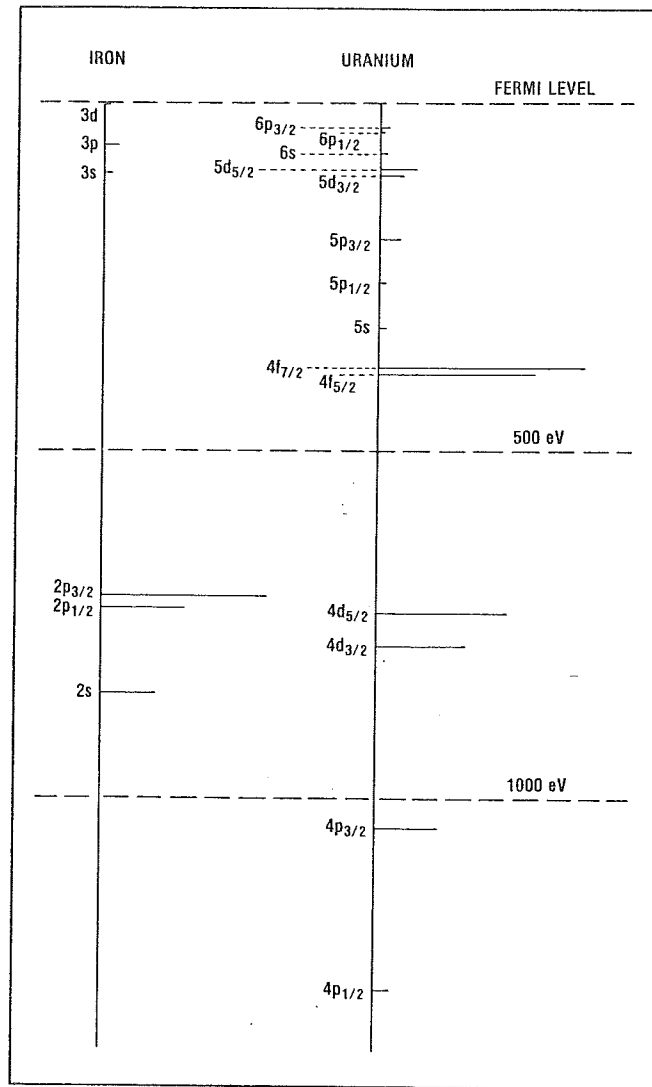


Figure 1. Relative ionization cross-sections and ionization energies for iron and uranium. (Line lengths are proportional to ionization cross-section and depths below Fermi level are proportional to ionization energy.)

$$E_{ki} + E_{pi} = E_{kf} + E_{pf}$$

$$E_{ki} = h\nu$$

$$E_{pi} = -eV$$

$$E_{kf} = E'_k$$

$$E_{pf} = 0$$

$$h\nu - eV = E_k + 0$$

$$h\nu = E'_k + eV$$

$$h\nu = E'_k + BE \leftarrow \text{isto je o elen. dugor ate'io Nivel Fermi}$$

$$E'_k + BE = E_k + BE + \phi$$

$$\therefore E'_k = E_k + \phi$$

$\begin{array}{l} \text{SUP.} \\ \uparrow \phi \\ \text{F.L.} \end{array}$
 $\begin{array}{l} E_k + BE + \phi \\ E_k + BE \end{array}$

$$\Rightarrow h\nu = E_k + BE + \phi$$

In addition to the photoelectrons emitted in the photoelectric process, Auger electrons are emitted due to relaxation of the energetic ions left after photoemission. This Auger electron emission occurs roughly 10^{-14} seconds after the photoelectric event. (The competing emission of a fluorescent x-ray photon is a minor process in this energy range, occurring less than one percent of the time.) In the Auger process, shown in Figure 2, an outer electron falls into the inner orbital vacancy, and a second electron is emitted, carrying off the excess energy. The Auger electron possesses kinetic energy equal to the difference between the energy of the initial ion and the doubly-charged final ion, and is independent of the mode of the initial ionization. Thus, photoionization normally leads to two emitted electrons, a photoelectron and an Auger

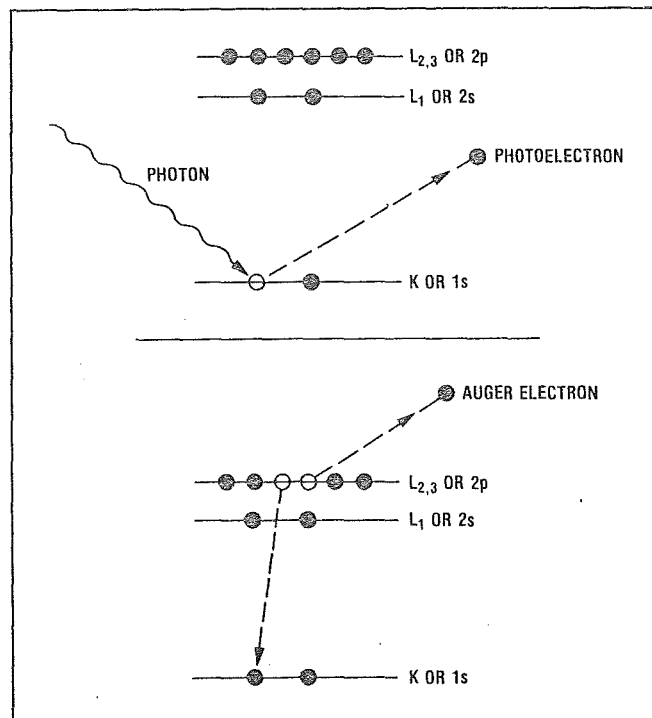


Figure 2. Diagram of the photoelectric process (top) and the Auger process (bottom).

electron. Of course, the energies of the electrons emitted cannot exceed the energy of the ionizing photons.

Probabilities of interaction of the electrons with matter far exceed those of the photons, so while the path length of the photons is of the order of micrometers, that of the electrons is of the order of tens of Angstroms. Thus, while ionization occurs to a depth of a few micrometers, only those electrons that originate within tens of Angstroms below the solid surface can leave the surface without energy loss. It is these electrons which produce the peaks in the spectra and are most useful. Those that undergo loss processes before emerging form the background. Experimental data

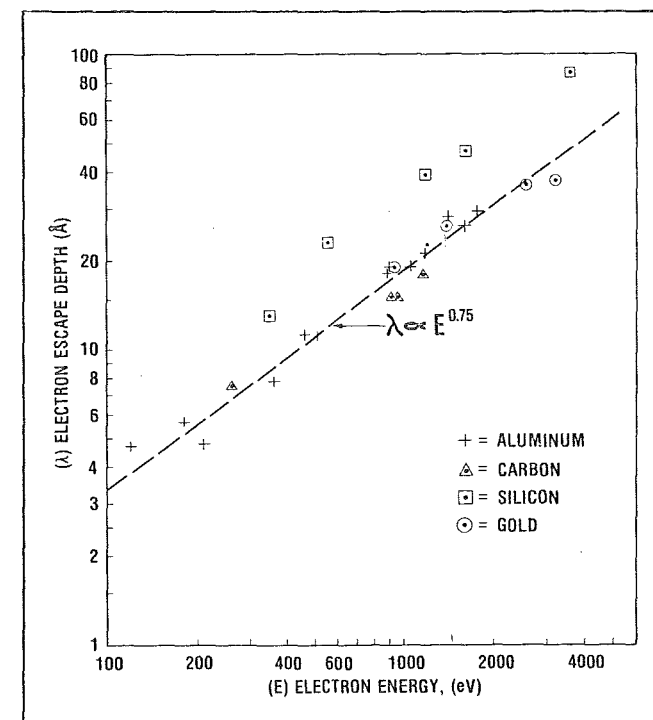


Figure 3. Electron mean free paths in various materials (from tabulation by C. J. Powell, Surface Science, 44 (1974) p. 29).

on mean free paths of electrons in various materials are shown in Figure 3.

The electrons leaving the sample are detected by an electron spectrometer according to their kinetic energy. The analyzer normally is operated as an energy "window", accepting only those electrons having an energy within the range of this fixed win-

dow, referred to as the pass energy. Scanning for different energies is accomplished by applying a variable electrostatic field, before the analyzer is reached. This retardation voltage may be varied from zero up to the photon energy. Electrons are detected as discrete events, and the number of electrons for a given detection time and energy is stored digitally or recorded using analog circuitry.

3. Preparing and Mounting Samples

In the majority of ESCA applications, sample preparation and mounting are not critical. Typically, the sample can simply be mechanically attached to the specimen mount and analysis begun, with the sample in the "as-received" condition. Sample preparation is even discouraged in many cases, especially where the natural surface is of interest, since almost any procedure will tend to modify surface composition. For those samples where special preparation or mounting procedures are necessary, the following techniques may be used.

A. REMOVAL OF VOLATILE MATERIAL.

Ordinarily any volatile material must be removed from the sample before analysis, although in exceptional cases, when the volatile layer is of interest, the sample may be cooled for analysis. Removal of volatile materials can be done by long-term pumping in a separate vacuum system or by washing with a suitable solvent. Samples can be washed efficiently in a Soxhlett extractor with a suitable solvent sufficiently volatile that it quickly evaporates from the sample after removal from the extractor. Choice of the solvent can be critical. Hexane or other light

hydrocarbon solvents are probably least likely to transform the surface, providing the solvent properties are satisfactory. It is desirable to do the extraction under a nitrogen atmosphere if the sample is likely to be sensitive to oxygen.

B. REMOVAL OF NON-VOLATILE ORGANIC CONTAMINANTS.

When the nature of an organic contaminant is not of interest, or when a contaminant obscures underlying inorganic material that is of interest, it may be removed in a Soxhlett extractor as described above. Freshly distilled solvent should be used to avoid the possibility of contamination by high boiling point impurities within the solvent.

C. SURFACE ETCHING.

Ion sputter-etching or other erosion techniques, such as the use of oxygen atoms on organic materials (see Section 1.5.E, p. 25), can also be used to remove surface contaminants. Argon ion etching is also commonly used to obtain information on composition as a function of depth into the specimen. It should be noted, however, that use of these methods for surface removal

are likely to change the chemical nature of the surface. Thus, identification of the remaining chemical states may not accurately reflect the initial composition.

D. ABRASION.

Abrasion of a surface can be accomplished without significant contamination by using silicon carbide paper #600. This does cause local heating, so that reaction with environmental gases may occur (e.g. oxidation in air and formation of nitrides in nitrogen). The roughness produced will reduce the ESCA signal intensity relative to that of a smooth sample. Use of this technique usually provides intense spectra of metals along with a contribution from the oxides and/or nitrides that form on the surface. Alkali and alkaline earth metals cannot be satisfactorily prepared in this manner. Spectra of such samples can be obtained only with rigorous ultra-high vacuum preparation and measurement conditions.

E. FRACTURE AND SCRAPING.

With proper equipment, many materials can be fractured or scraped within the test chamber under ultra-high vacuum conditions. While this obviates contamination by reaction with atmospheric gases, attention must nevertheless be given to unexpected results that can occur. When fracturing, the fracture might occur along grain boundaries, for example, and scraping can cover hard material with soft material when the system is multi-phase.

F. GRINDING TO POWDER.

Spectra reasonably characteristic of bulk composition are most frequently obtained on samples ground to a powder in an alumina mortar. Harder surfaces than alumina can be used, but they are expensive for general use. Again, protection of the fresh surfaces from the atmosphere is required. When grinding samples,

localized high temperatures can also be produced, so grinding should be done slowly to minimize chemical change at the newly created surfaces. The alumina mortar should be well-cleaned before re-use, preferably ending with a concentrated nitric acid cleaning, followed by rinsing with distilled water, and thorough drying.

G. MOUNTING POWDERS FOR ANALYSIS.

There are a number of methods that can be used to mount powders for analysis. Perhaps the most widely used method is to carefully and lightly dust the powder on polymer film based adhesive tape with a camel's hair brush. The powder must be dusted on lightly, with no wiping strokes across the powder surface. Many researchers shun organic tape for UHV work, but certain types have been used successfully in the 10^{-9} Torr range.

Alternative methods for mounting powders include pressing the powder into an indium foil, supporting the powder on a metallic mesh, pressing the powder into pellets, and simply depositing the powder by gravity. With the indium foil method, the powder is pressed between two pieces of pure foil. The pieces are then separated and one of them mounted for analysis. Success with this technique has been varied. Sometimes bare indium remains exposed and, if the sample is an insulator, parts of the powder can charge differently from other parts. Differential charging can also be a problem when a metallic mesh is used to support the powder. If a press is used to form the powder into a pellet of workable dimensions, a press with hard and extremely clean working surfaces should be used. If a specimen holder with a horizontal sample surface is used, the powder can simply be deposited by gravity in a uniform layer. With this method, care must be taken in pumpdown to ensure that gas evolution does not disturb the powder.

H. CONSIDERATIONS OF MOUNTING ANGLE.

In ESCA studies the sample mounting angle is not critical, but it does have some effect on the spectra. The use of a shallow electron take-off angle accentuates the spectrum of any layer segregated on the surface, whereas a sample mounting angle normal to the analyzer axis minimizes the contribution from such a layer. This effect can be utilized in estimating the depth of atoms contributing to the spectrum. It is not limited to planar surfaces, but is even observed with powders, though the effects are muted. The geometry of the double pass cylindrical-mirror analyzer used to obtain the

spectra presented in this Handbook effectively integrates over a large range of take-off angles when used in the normal configuration. This reduces the effect of variations in sample geometry and mounting angle to an insignificant level in most cases. However, use of a 50° sample mounting angle in conjunction with the angle-resolved aperture inside the analyzer allows the take-off angle to be varied without changing the sample mounting angle. Thus, take-off angle effects can be minimized for routine work, or emphasized when desired (see Section I.5.E., p. 25)

4. Experimental Procedure

A. EXPERIMENTAL TECHNIQUE FOR OBTAINING SPECTRA.

All spectra in this Handbook were obtained using a PHI Model 550 ESCA/SAM system. A schematic diagram of the apparatus, shown in Figure 4, indicates the relationship of major components, including the electron energy analyzer, the x-ray source, and the ion gun used for sputter-etching. The Model 25-260, Precision Electron Energy Analyzer, incorporated in the ESCA/SAM is a double pass, cylindrical-mirror type analyzer (CMA) with a retarding grid input stage. The x-ray source is a standard flange-mounted Physical Electronics source which can be configured with a magnesium or an aluminum anode. All of the spectra in the Handbook were taken with an x-ray source power of 600 watts (10Kv-60 ma). As shown in Figure 4, the specimens were mounted on the end of the sample introduction probe at an angle of 50° with

respect to the analyzer axis. The x-ray source is located perpendicular to the analyzer axis and the ion beam is nearly normal to the sample surface.

In the ESCA/SAM System, energy distribution, energy resolution and the size of the analysis area are strictly a function of the analyzer. For all of the spectra in the Handbook the analyzer was operated in the retarding mode. This gives an energy distribution function with intensity proportional to E^{-1} . The retarding grids are used to scan the spectrum while the CMA is operated at a constant pass energy. This results in constant resolution (ΔE) across the entire energy spectrum. The size of the analysis area is defined by the size of the circular apertures at the output of the CMA stages. Analyzer energy resolution ($\Delta E/E$) is also determined by these apertures. In the Precision Electron Energy

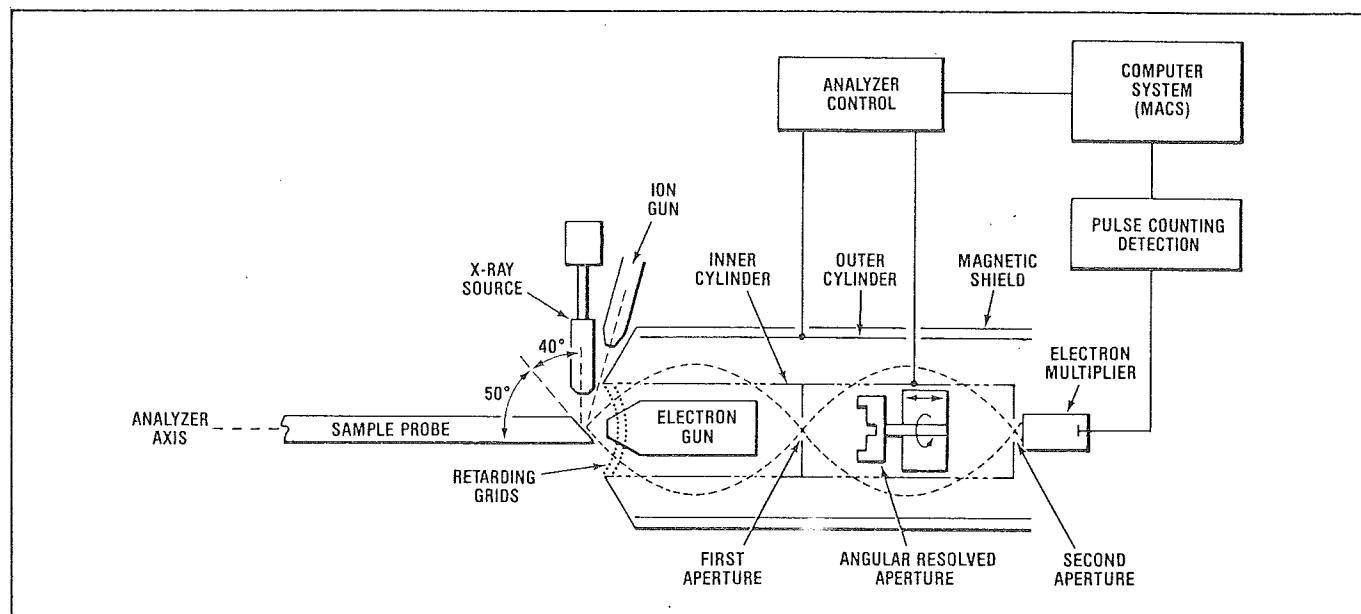


Figure 4. Schematic representation of the PHI Model 550, ESCA/SAM system.

Analyzer, three different aperture sizes are available. All spectra in the Handbook were obtained using the largest apertures. Use of the large apertures results in maximum signal intensity, a circular analysis area approximately 5mm in diameter, and energy resolution which is 2% of the pass energy.

All spectra obtained while compiling the data for the Handbook were recorded and stored using a PHI Multiple-technique Analytical Computer System. The instrument was calibrated weekly and the calibration was checked several times each day during data acquisition. The analyzer work function was determined assuming the binding energy of the gold $4f_{7/2}$ peak to be 83.8 eV. All survey spectra, scans of 1000 eV or more, were taken at a pass energy of 50 eV, providing an instrumental resolution of 1 eV. The narrow scans of strong lines are, in most cases, just wide enough to encompass the peak(s) of

interest and were obtained with a pass energy of 25 eV. The narrow spectra are necessary to determine accurately the energy and shape of the strong lines. On insulating samples, a high resolution spectrum of the adventitious hydrocarbon on the surface of the sample was taken to use as a reference for charge correction. It has been experimentally determined that the binding energy for the adventitious carbon peak is approximately 284.6 eV.

The samples analyzed to obtain the spectra in the handbook were standard materials of known composition. Metal foils and polycrystalline materials with large surface areas were mechanically held to the specimen probe. Powder samples were ground with a mortar and pestle to expose fresh surfaces and dusted onto adhesive tape. Most elemental standards were sputter-etched immediately prior to analysis to remove surface contaminants. Most com-

pounds, however, were ground and the freshly exposed surface was analyzed without etching in order to avoid possible changes in surface chemistry. Several materials, for example mercury, were cooled for the analysis, and xenon and argon were imbedded in graphite via ion implantation just prior to analysis.

B. INSTRUMENT CALIBRATION.

To ensure the accuracy of the data presented in the Handbook, the instrument used to obtain the data was calibrated regularly throughout the data gathering process. The energy scale was periodically calibrated using a high precision digital voltmeter. Then, several times each day, the calibration was checked for accuracy.

The best way to check the calibration, and the method used here, is to record suitable lines from a known, conducting specimen. Typically, the Au4f or Cu2p and 3p lines are used. The lines should be recorded with a narrow sweep width in the range of 5-10 eV, and a pass energy of 25 eV or less, corresponding to the pass energy normally used for high resolution scans, should be used. The peak position is determined accurately by drawing cords parallel to the baseline and drawing the best straight line or simple monotonic curve through the midpoints, as shown in Figure 5. The peaks should occur at exactly the correct position in the spectrum.

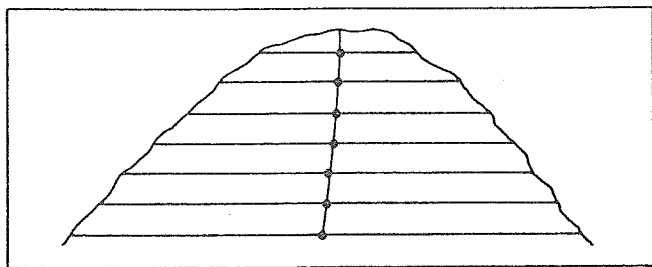


Figure 5. Method for accurately locating the peak position from a narrow scan.

There is not as yet general agreement on accurate values of any standard line energies, but at this point the following is recommended for clean gold and copper (on a binding energy scale):

Cu2p _{3/2}	932.4 eV
Cu (L ₃ M ₅ M ₅)	567.9 eV (Al radiation)
	334.9 eV (Mg radiation)
Cu3p _{3/2}	74.9 eV
Au4f _{7/2}	83.8 eV

Since the 2p_{3/2} and 3p_{3/2} photoelectron peak energies of copper are widely separated in energy, measurement of these peak binding energies provides a quick and simple means of checking the magnitude of the binding energy scale. Utilizing all of the above standard energies establishes the magnitude and linearity of the energy scale and its position, i.e., the location of the Fermi level.

C. PROGRAMMING SCANS FOR AN UNKNOWN SAMPLE.

For a typical ESCA investigation where the surface composition is unknown, a broad scan survey spectrum should be obtained first to identify the elements present. Once the elemental composition has been determined, narrower detailed scans of selected peaks can be used for a more comprehensive picture of the chemical composition. This is the procedure that has been followed in compiling data for the Handbook, even though specimen composition was known prior to analysis.

- (1) Survey Scans. Ordinarily, a scan range from 1000-0 eV binding energy is sufficient for the identification of all detectable elements. In a few cases, such as with Zn, Mg, and Na, the strongest lines may occur at a binding energy above this range. Most spectra in this Handbook were recorded with scan ranges of 1000-0 or 1100-0 eV binding energy. There are

a few, especially where $AlK\alpha$ x-rays were used, that cover a wider range. In an unknown sample, if specific elements are suspected at low concentrations, their standard spectra should be consulted before programming the survey scan. If the strongest line occurs above 1000 eV binding energy, the scan range can be modified accordingly.

An analyzer pass energy of 100 eV, in conjunction with the normal ESCA aperture settings, is recommended for survey scans with the ESCA/SAM system. These settings result in adequate resolution ($\Delta E = 2\text{eV}$) for elemental identification and produce very high signal intensities, minimizing data acquisition time and maximizing elemental detectability.

(2) Detail Scans. For purposes of chemical state identification, for quantitative analysis of minor components and for peak deconvolution and other mathematical manipulations of the data, detail scans must be obtained for precise peak location and for accurate registration of line shapes. There are some logical rules for this programming:

i. Scans should be wide enough to encompass the background on both sides of the region of interest, yet narrow enough, less than 25 eV, to permit determination of the exact position of the peaks. If these requirements cannot be met in one region, two regions of the spectrum must be programmed. Sufficient scanning must be done, within the time limitations of the

analysis, to obtain good counting statistics and clear spectra.

ii. Peaks from any species thought to be radiation-sensitive or transient should be run first. Otherwise any convenient order may be chosen.

iii. If the $C1s$ line is to be used for charge referencing, it should preferably be run early and again late in the sequence or, alternatively, run at a time closest to the region of greatest interest. This is because there is occasionally a slight change in steady-state static charge with time (cf Section I.5.C., p. 17).

iv. No clear guidelines can be given on the maximum duration of data gathering on any one sample. It should be recognized, however, that chemical states have vastly varying degrees of radiation sensitivity, and for any one set of irradiation conditions there exists for many samples a period beyond which it is impractical to attempt to gather data.

v. With the ESCA/SAM, an analyzer pass energy of 25 eV ($\Delta E = 0.5\text{eV}$) is normally adequate for routine detail scans. Where higher resolution is needed, lower pass energies can be utilized with corresponding loss of signal intensity. For the ultimate in resolution, the smaller apertures should be used in conjunction with an analyzer pass energy of 10 or 15 eV.

5. Data Interpretation

A. THE NATURE OF THE SPECTRUM

(1) General Features. The spectrum is displayed as a plot of electron binding energy versus the number of electrons in a fixed, small energy interval. The position on the kinetic energy scale equal to the photon energy minus the spectrometer work function corresponds to a binding energy of zero with reference to the Fermi level (equation 1). Therefore, a binding energy scale beginning at that point and increasing to the left is customarily used.

The spectra in this Handbook are typical for the various elements. The well-defined peaks are due to electrons that have not lost energy in emerging from the sample. Electrons that have lost energy form the raised background at binding energies higher than the peaks. The background is continuous because the energy loss processes are random and multiple.

The "noise" in the spectrum is not instrumental, but is the consequence of the collection of single electrons as counts randomly spaced in time. The standard deviation for counts collected in any channel is equal to the square root of the counts, so that the percent standard deviation is $100/(\text{counts})^{1/2}$. The signal/noise ratio is then proportional to the square root of the counting time. The background level upon which the peak is superimposed is a characteristic of the specimen and the transmission characteristics of the instrument.

(2) Kinds of Lines. Several types of peaks are observed in ESCA spectra. Some are fun-

damental to the technique, and are always observed. Others are dependent upon the exact physical and chemical nature of the sample. The following describes the various spectral features that are likely to be encountered.

i. Photoelectron Lines. The most intense of the photoelectron lines are usually relatively symmetrical and are typically the narrowest lines observed in the spectrum. Photoelectron lines of pure metals can, however, exhibit considerable asymmetry due to coupling with conduction electrons. Peak width is a convolution of the natural line width, the width of the x-ray line and the instrumental contribution to the line width. Less intense photoelectron lines at higher binding energies are usually wider by 1-4 eV than the lines at lower binding energies. All of the photoelectron lines of insulating solids are of the order of 0.5 eV wider than photoelectron lines of conductors. The approximate binding energies of all photoelectron lines detectable are catalogued in Tables 1-4 of the Appendix.

ii. Auger Lines. These are, more properly, groups of lines in rather complex patterns. There are four main Auger series observable in ESCA. They are the KLL, LMM, MNN, and NOO series, identified by specifying the initial and final vacancies in the Auger transition. The KLL series, for example, includes those processes with an initial vacancy in the K shell and final double vacancy in the L shell. The symbol V, e.g. KVV, indicates that the final vacancies are in valence levels. The KLL series has, theoretically, nine lines and others have

still more. Since Auger lines have kinetic energies that are independent of the ionizing radiation they appear on a binding energy plot to be in different positions when ionizing photons of different energy (i.e. different x-ray sources) are used. Core-type Auger lines (with final vacancies deeper than the valence levels) usually have at least one component of intensity and width similar to the most intense photoelectron line. Positions of the more prominent Auger components are catalogued along with the photoelectron peaks in Tables 1 through 4 in the Appendix.

- iii. X-ray Satellites. The x-ray emission spectrum used for irradiation exhibits not only the characteristic x-ray, but some minor x-ray components at higher photon energies. For each photoelectron peak that results from the $K\alpha$ x-ray photons, there is a family of minor peaks at lower binding energies, with intensity and spacing characteristic of the x-ray anode material. The pattern of such satellites for Mg and Al is shown in Figure 6 and Table 1.

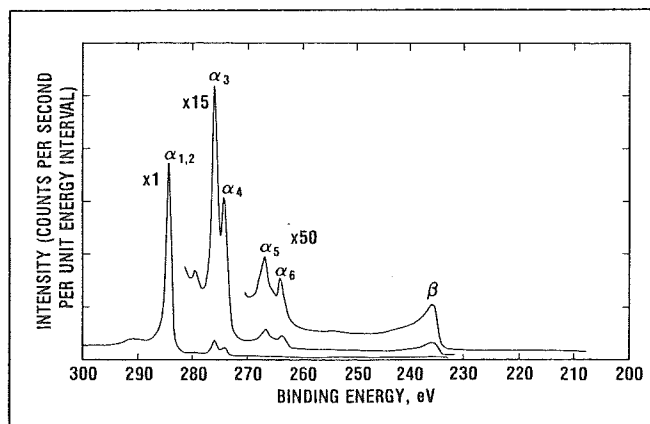


Figure 6. Mg x-ray satellites (C1s graphite spectrum).

Table 1 — X-ray satellite energies and intensities

		$\alpha_{1,2}$	α_3	α_4	α_5	α_6	β
Mg	displacement, eV	0	8.4	10.2	17.5	20.0	48.5
	relative height	100	8.0	4.1	0.55	0.45	0.5
Al	displacement, eV	0	9.8	11.8	20.1	23.4	69.7
	relative height	100	6.4	3.2	0.4	0.3	0.55

- iv. X-ray "Ghosts". Occasionally x-radiation from an element other than the x-ray source anode material impinges upon the sample, resulting in small peaks corresponding to the most intense spectral peaks, but displaced by a characteristic energy interval. These lines can be due to Mg impurity in the Al anode, or vice versa, Cu from the anode base structure or generation of x-ray photons in the aluminum foil x-ray window. On occasion, such lines can originate via generation of x-rays within the sample itself. This last possibility is rare, because the probability of x-ray emission is low relative to the Auger transition. Nevertheless, such minor lines can be puzzling. Table 2 indicates where such peaks are most likely to occur, relative to the most intense photoelectron lines. Since the appearance of "ghost" lines is a rare occurrence, they should not be considered in line identification until all other possibilities are excluded.

Table 2 — Displacements of x-ray "ghost" lines

(Apparent binding energy of the "ghost" line minus that of the parent photoelectron line.)

Contaminating Radiation	Anode Material	
	Mg	Al
O ($K\alpha$)	728.7	961.7
Cu ($L\alpha$)	323.9	556.9
Mg ($K\alpha$)	—	233.0
Al ($K\alpha$)	-233.0	—

v. Shake-Up Lines. Not all photoelectric processes are simple ones, leading to the formation of ions in the ground state. Rather often, there is a finite probability that the ion will be left in an excited state, a few electron volts above the ground state. In this event, the kinetic energy of the emitted photoelectron is reduced, with the difference corresponding to the energy difference between the ground state and the excited state. This results in the formation of a satellite peak a few electron volts lower in kinetic energy (higher in binding energy) than the main peak. As an example, the characteristic shake-up line for carbon in unsaturated compounds, a shake-up process involving the energy of the $\pi \rightarrow \pi^*$ transition, is shown in Figure 7.

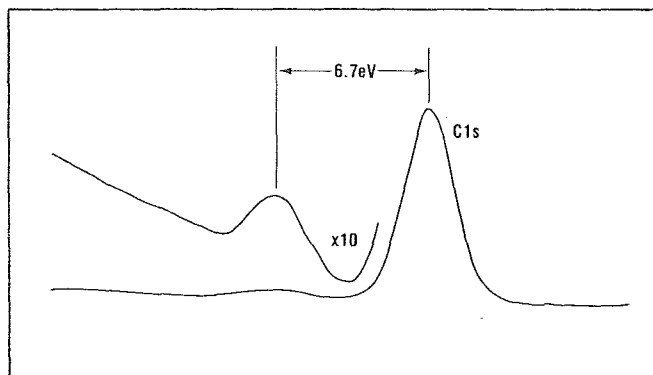


Figure 7. The π -bond shake-up satellite for the C1s line in polystyrene.

In some cases, most often with paramagnetic compounds, the intensity of the shake-up satellite may approach that of the main line. More than one satellite of a principal photoelectron line can also be observed, as shown in Figure 8. The occurrence of such lines is sometimes more apparent in Auger spectral contours, of which

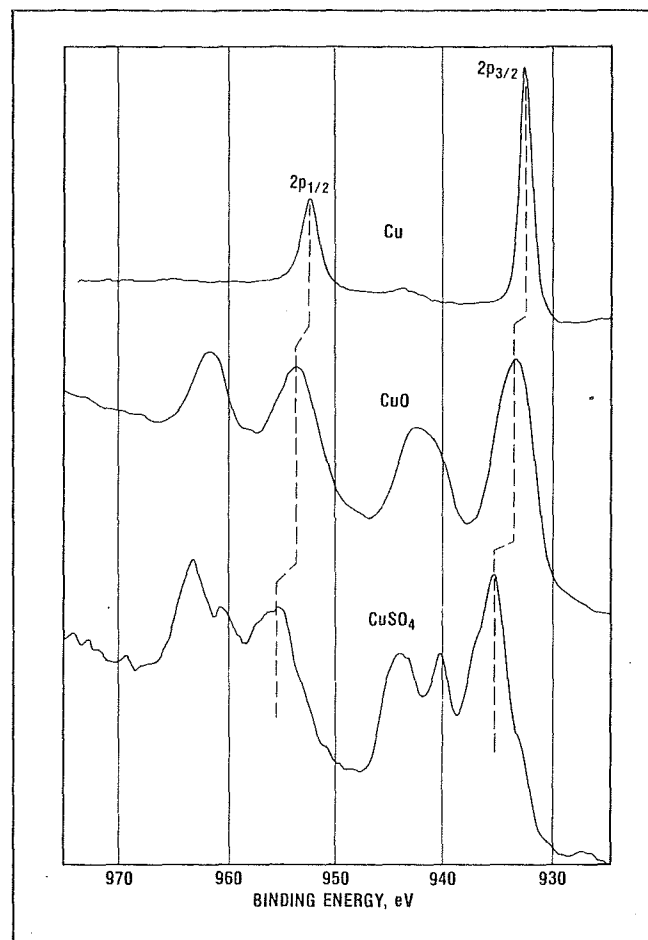


Figure 8. Examples of shake-up lines observed with the copper 2p spectrum.

an example is presented in Figure 9. The displacements and relative intensities of shake-up satellites can sometimes be useful in identifying the chemical state of an element, as discussed in Section I.5.C., p. 20.

vi. Multiplet Splitting. Emission of an electron from a core level of an atom that itself has a spin (unpaired electrons in valence levels)

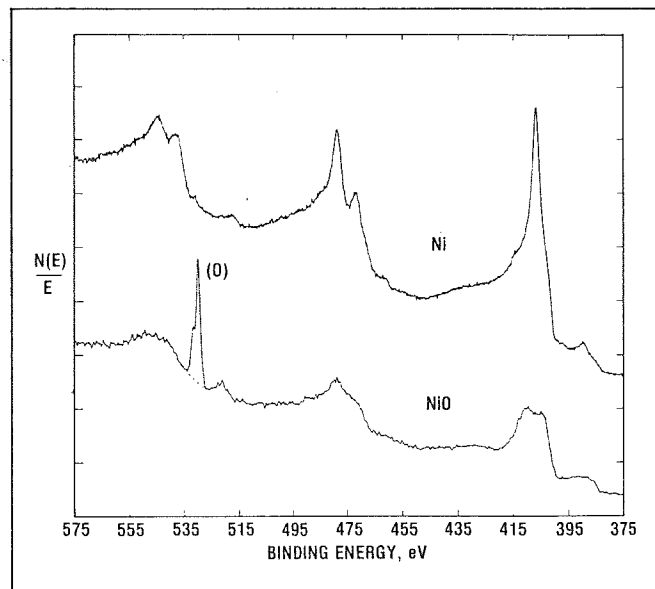


Figure 9. Some effects of chemical state on Auger line shapes.

can create a vacancy in two or more ways. The coupling of the new unpaired electron left after photoemission from an s-type orbital with other unpaired electrons in the atom can create an ion with either of two configurations and two energies. This results in a photoelectron line that is split asymmetrically into two components similar to the one shown in Figure 10.

Splitting also occurs in the ionization of p levels, but the result is more complex and subtle. In favorable cases, it results in an apparent slight increase in the spin doublet separation, evidenced in the separation of the $2p_{1/2}$ and $2p_{3/2}$ lines in first row transition metals, and the generation of a less easily noticed asymmetry in the line shape of the components. Often such effects on the p doublet are obscured by shake-up lines.

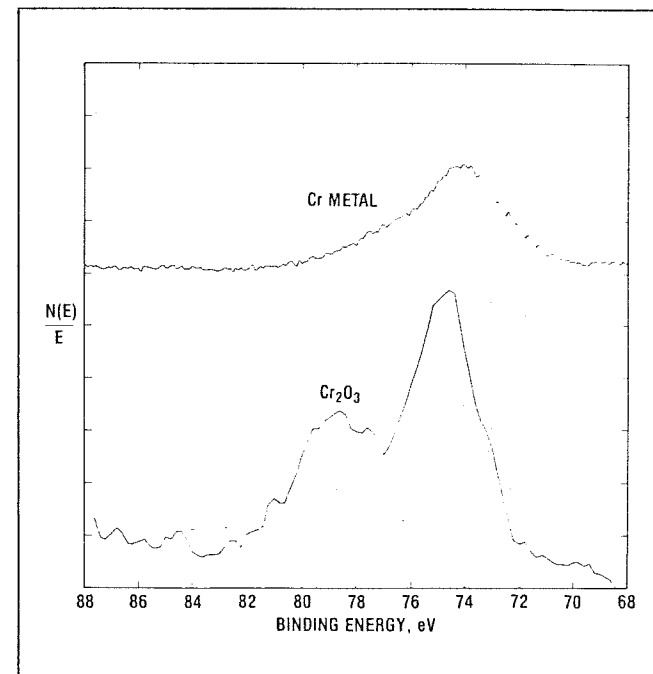


Figure 10. Multiplet splitting in the Cr 3s line.

vii. Energy Loss Lines. With some materials, there is an enhanced probability for loss of a specific amount of energy due to interaction between the photoelectron and other electrons in the surface region of the sample. An example of this is shown in Figure 11. The enhanced probability of energy loss produced a distinct and rather sharp hump at an energy about 21 eV above the binding energy of the parent line. Under certain conditions of spectral display, energy loss lines can cause confusion. Such phenomena in insulators are rarely sharper than that shown in Figure 11, and are usually much more muted. They are, of course, different in each solid medium.

With metals, the effect is often much more dramatic, as indicated by the loss lines for

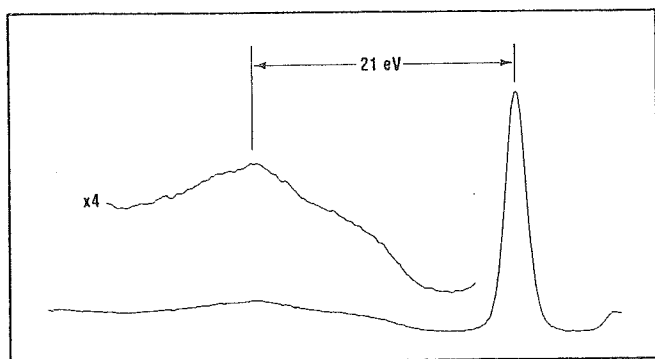


Figure 11. Energy loss envelope from the O1s line in SiO_2 .

aluminum shown in Figure 12. Energy loss to the conduction electrons occurs in well-defined quanta characteristic of each metal. The photoelectron line, or the Auger line, is successively mirrored at intervals of higher binding energy, with reduced intensity. The energy interval between the primary peak and the loss peak is called the plasmon energy. The so-called "bulk

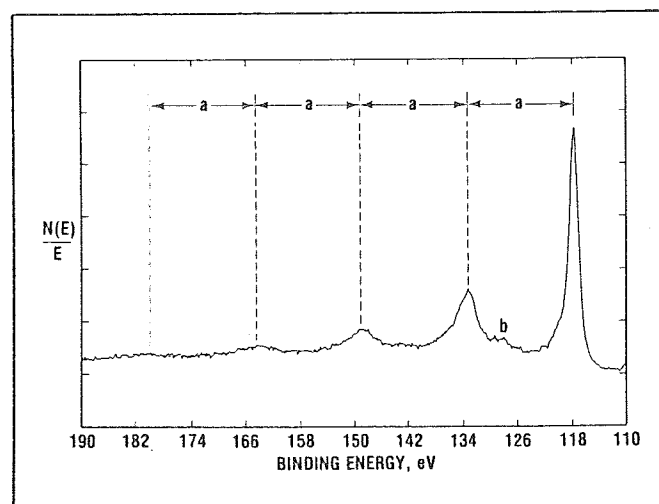


Figure 12. Energy loss (plasmon) lines associated with the 2s line of aluminum ($a = 15.3\text{eV}$; note surface plasmon at b).

plasmons" are the more prominent of these lines. A second series, the "surface plasmons", exists at energy intervals determined by dividing the bulk plasmon energy by $\sqrt{2}$. The effect is not easily observable in non-conductors, nor is it prominent in all conductors.

viii. Valence Lines and Bands. Lines of low intensity occur in the low binding energy region of the spectrum between the Fermi level and about 10-15 eV binding energy. These lines are produced by photoelectron emission from molecular orbitals and from solid state energy bands. Differences between insulators and conductors are especially noted by the absence or presence of electrons from conduction bands at the Fermi level.

B. LINE IDENTIFICATION

In general, interpretation of the ESCA spectrum is most readily accomplished by first identifying the lines that are almost always present, specifically those of carbon and oxygen, then identifying major lines and associated weaker lines and, lastly, identifying the remaining weak lines. The following step-by-step procedure generally simplifies the data interpretation task and minimizes data ambiguities.

Step 1. The C1s, O1s, C(KLL) and O(KLL) lines are usually prominent in any spectrum. Identify these lines first along with all derived x-ray satellites and energy loss envelopes.

Step 2. Identify other intense lines (cf Appendix Tables) present in the spectrum. Then label any related satellites and other less intense spectral lines associated with those elements. Keep in mind that some lines may be interfered with by more intense, overlapping lines from other elements. The most

serious interferences by the carbon and oxygen lines, for example, are Ru3d by C1s, V2p and Sb3d by O1s, I(MNN) and Cr(LMM) by O(KLL), and Ru(MNN) by C(KLL).

Step 3. Identify any remaining minor lines. In doing this, assume they are the most intense lines of an unknown element. If not, they should already have been identified in previous steps. Again, possible line interferences should be kept in mind. Small lines that seem unidentifiable can be ghost lines. This possibility can be checked for the more intense parent photoelectron lines using Table 2 (p. 13).

Step 4. Check the conclusions by noting the spin doublets for p, d, and f lines. They should have the right separation (cf Appendix Tables 1 and 2, pp. 182 and 184) and should be in the correct intensity ratio. The ratio for p lines should be about 1:2, d lines 2:3, and f lines 3:4 except that p lines, especially 4p lines, may be less than 1:2.

C. CHEMICAL STATE IDENTIFICATION

The identification of chemical states depends primarily upon the accurate determination of line energies. To determine line energies accurately, the voltage scale of the instrument must be precisely calibrated (cf Section I.4.B., p. 10), a line with a narrow sweep range must be recorded with good statistics (of the order of several thousand counts per channel above background), and accurate correction must be made for static charge if the sample is an insulator.

(1) Determination of Static Charge on Insulators.

During analysis, insulating samples tend to acquire a steady-state charge of as much as several volts. This steady-state charge is a balance between electron loss from the sur-

face by emission and electron gain by conduction or by acquisition of slow or thermal electrons from the vacuum space. The steady-state charge, usually positive, can be minimized by adding slow electrons to the vacuum space with an adjacent neutralizer or flood gun. It is often advantageous to do this to reduce differential charging and to sharpen the spectral lines.

A serious problem is the exact determination of the extent of charging. Any positive charging adds to the retardation and tends to make the peaks appear at higher binding energy, whereas excessive compensation can make the peaks shift to lower binding energy. The following are five methods that are usually valid for charge correction on insulating samples:

i. Measurement of the position of the C1s line from adventitious hydrocarbon nearly always present on samples introduced from the laboratory environment or from a glove box. This line, on unsputtered inert metals such as gold or copper, appears at 284.6 eV, so any shift from this value can be taken as a measure of the static charge. (Much of the literature uses the more approximate value of 285). At this time, it is not known whether a reproducible line position exists for carbon remaining on the surface after ion beam etching.

ii. Evaporation of a trace of gold onto the sample after the spectra have been recorded. The Au4f doublet is then recorded as well as a repetition of the most important line in the sample spectrum. It is then assumed that the potential of the gold islands reflects the new steady-state charge of the surface of the sample. Care

must be taken to ensure that the gold is present in trace quantities so that the original spectrum is little affected. In this procedure there may well be a double correction. The steady-state potential after gold is deposited may well be different from the steady-state potential in the original sample before gold deposition.

iii. The use of an internal standard, such as a hydrocarbon moiety in the sample. The value of 284.6 eV for the C1s line is recommended.

iv. The use of an insulating sample so thin that it effectively does not insulate. This can be assumed if the spectrum of the underlying conductor appears in good intensity and line positions are not affected by changes in electron flux from the charge neutralizer.

v. For the study of supported catalysts or similar materials, one can adopt a suitable value for a constituent of the support and use that to interrelate binding energies of different samples. One must be certain that treatments of the various samples are not so different that the inherent binding energies of support constituents are changed.

Some precautions should be borne in mind. If the sample is heterogeneous on even a micrometer scale, particles of different materials can charge to different extents, and interpretation of the spectrum is complicated accordingly. One cannot physically mix a conducting standard like gold or graphite of micron dimensions with a powder and validly use the gold or graphite line in order to correct for static charge.

(2) Photoelectron Line Chemical Shifts and Separations. An important advantage of ESCA is the ability to obtain information on chemical states from the variations in binding energies, or chemical shifts, of the photoelectron lines. This has been extremely useful in many studies. While many attempts have been made to calculate chemical shifts and absolute binding energies, the factors involved, especially in the solid state, are imperfectly understood and one must rely on experimental data on standard materials. The tables accompanying the spectra in this Handbook record considerable data from the literature as well as data obtained specifically for this Handbook. All literature data have been carefully evaluated and corrected, and are believed reliable.^(a) These data have been adjusted to the instrumental calibration and static charge reference values given above, and are, therefore, directly comparable.

Since occasional line interferences do occur, it is sometimes necessary to use a line other than the most intense one in the spectrum. Chemical shifts are very uniform among the photoelectron lines of an element, so that line separations rarely vary by more than 0.2 eV. However, exceptional separations can occur in paramagnetic materials because of multiplet splitting. Separations of photoelectron lines can be determined approximately from Tables 1 and 2 in the Appendix (pp. 182 and 184).

(3) Auger Line Chemical Shifts and the Auger Parameter. Core-type Auger lines (transitions

(a) In some cases, different binding energy values appearing in the literature for the same material could not be reconciled, and no grounds could be found for choosing one over the other. In such cases, more than one value is included to indicate the degree of uncertainty.

ending with double vacancies below the valence levels) usually have at least one component that is narrow and intense, often nearly as intense as the strongest photoelectron line (cf. spectra for F, Na, As, In, Te, and Pb). There are four core Auger groups that can be generated by Mg or Al x-rays: the KLL (Na, Mg); the LMM (Cu, Zn, Ga, Ge, As, and Se); the MNN (Ag, Cd, In, Sn, Sb, Te, I, Xe, Cs, and Ba); and the NOO (Au, Hg, Tl, Pb, and Bi). The MNN lines in the rare earths, while accessible, are very broad because of multiplet splitting and shake-up phenomena with most of the compounds. Valence-type Auger lines (final states with vacancies in valence levels), such as those for O and F (KLL); Mn, Fe, Co, and Ni (LMM); and Ru, Rh, and Pd (MNN), can be intense and are, therefore, also useful. Chemical shifts occur with Auger lines as well as with photoelectron lines. The chemical shifts are different from those of the photoelectron lines, however, and usually are considerably more pronounced. This can be very useful for identification of chemical states, especially in combination with photoelectron chemical shift data. If data for the various chemical states of an element are plotted, with the kinetic energy of the photoelectron line on the abscissa and that of the Auger line on the ordinate, a two-dimensional chemical state plot is obtained. Such plots accompany the spectra for F, Na, Cu, Zn, As, Ag, Cd, In, and Te.

With chemical states displayed in two dimensions, the method becomes more powerful as a tool for identifying the chemical components. In the format adopted for the Handbook, the kinetic energy of the Auger line is plotted against the binding energy of the photoelectron line, with the latter plotted in the -x direction (kinetic energy is still, im-

plicitly, +x). the kinetic energy of the Auger electron, referred to the Fermi level, is easily calculated by subtracting from the photon energy the position of the Auger line on the binding energy scale.

With this arrangement, each diagonal line represents all values of equal sums of Auger kinetic energy and photoelectron binding energy. A quantity called the Auger parameter, α , is defined as,

$$\alpha = KE_A - KE_p = BE_p - BE_A \quad (2)$$

or, the difference in binding energy between the photoelectron and Auger lines. This difference can be accurately determined because static charge corrections cancel. Then, with all kinetic energies and binding energies referenced to the Fermi level,

$$KE_p = h\nu - BE_A \quad (3)$$

$$KE_A + BE_p = h\nu + \alpha \quad (4)$$

or, the sum of the kinetic energy of the Auger line and the binding energy of the photoelectron line equals the Auger parameter plus the photon energy. A plot showing Auger kinetic energy versus photoelectron binding energy then becomes independent of the energy of the photon.

In general, polarizable materials, especially conductive materials, have a high Auger parameter, while insulating compounds fall lower on the grid. The points on the two-dimensional plot are drawn as rectangular boxes at 45°, reflecting the expected error of measurement in the two perpendicular directions. At present, sufficient data for the two-dimensional chemical state plots are available only for the nine elements listed above.

(4) Chemical Information From Satellite Lines and Peak Shapes.

i. Shake-up Lines. These satellite lines have intensities and separations from the parent photoelectron line that are unique to each chemical state (Figure 8). Some Auger lines also exhibit radical changes with chemical state that reflect these processes (Figure 9). With transition elements and rare earths the absence of shake-up satellites is usually characteristic of the elemental or

diamagnetic states. Prominent shake-up patterns typically occur with paramagnetic states. Table 3 has been included as a guide to some expected paramagnetic states.

ii. Multiplet Splitting. On occasion, the multiplet splitting phenomenon can also be helpful in identifying chemical states. The 3s lines in the first series of transition metals, for example, exhibit separations characteristic of each paramagnetic

Table 3 — General guide to paramagnetic species

Multiplet splitting and shake-up lines are generally expected in the paramagnetic states below.

Atomic No.	Paramagnetic States	Diamagnetic States
22	Ti ⁺² , Ti ⁺³	Ti ⁺⁴
23	V ⁺² , V ⁺³ , V ⁺⁴	V ⁺⁵
24	Cr ⁺² , Cr ⁺³ , Cr ⁺⁴ , Cr ⁺⁵	Cr ⁺⁶
25	Mn ⁺² , Mn ⁺³ , Mn ⁺⁴ , Mn ⁺⁵	Mn ⁺⁷
26	Fe ⁺² , Fe ⁺³	K ₄ Fe(CN) ₆ , Fe(CO) ₄ Br ₂
27	Co ⁺² , Co ⁺³	CoB, Co(NO ₂) ₃ (NH ₃) ₃ , K ₃ Co(CN) ₆ , Co(NH ₃) ₆ Cl ₃
28	Ni ⁺²	K ₂ Ni(CN) ₄ , square planar complexes
29	Cu ⁺²	Cu ⁺¹
42	Mo ⁺⁴ , Mo ⁺⁵	Mo ⁺⁶ , MoS ₂ , K ₄ Mo(CN) ₈
44	Ru ⁺³ , Ru ⁺⁴ , Ru ⁺⁵	Ru ⁺²
47	Ag ⁺²	Ag ⁺¹
58	Ce ⁺³	Ce ⁺⁴
59-70	Pr, Nd, Sm, Eu, Gd, Tb, Dy, Ho, Er, Tm, Yb compounds	
74	W ⁺⁴ , W ⁺⁵	W ⁺⁶ , WO ₂ , WCl ₄ , WC, K ₄ W(CN) ₈
75	Re ⁺² , Re ⁺³ , Re ⁺⁴ , Re ⁺⁵ , Re ⁺⁶	Re ⁺⁷ , ReO ₃
76	Os ⁺³ , Os ⁺⁴ , Os ⁺⁵	Os ⁺² , Os ⁺⁶ , Os ⁺⁸
77	Ir ⁺⁴	Ir ⁺³
92	U ⁺³ , U ⁺⁴	U ⁺⁶

chemical state. The 3s line, however, is weak and therefore is not often useful analytically. The 2p doublet separation is also affected by multiplet splitting and the lines are more intense. The effect becomes very evident with cobalt compounds where the separation varies up to one electron volt. Little utilization of this effect has yet been made. However, when first row transition metal compounds are under study, it may prove useful to record accurately these line separations and make comparisons with model compounds.

iii. Auger Line Shape. Valence type Auger transitions form final-state ions with vacancies in molecular orbitals. The distribution of the group of lines is strongly affected, therefore, by the nature of the molecular orbitals in the different chemical states. Although little has yet been published on this subject, the spectroscopist should bear in mind the possible utility of Auger line shapes of oxygen, fluorine, the first row transition metals (Sc-Ni), and Ru, Rh, and Pd.

D. QUANTITATIVE ANALYSIS

For many ESCA investigations, it is important to determine the relative concentrations of the various constituents. Methods for quantifying the ESCA measurement utilizing peak area sensitivity factors and peak height sensitivity factors have been developed. The method which utilizes peak area sensitivity factors typically is the more accurate and is discussed below. The method for determining peak height and peak area is shown in Figure 13. This approach is satisfactory for quantitative work except with transition metal spectra with prominent shake-up lines. For these, it is often better to include the entire 2p region when measuring peak area.

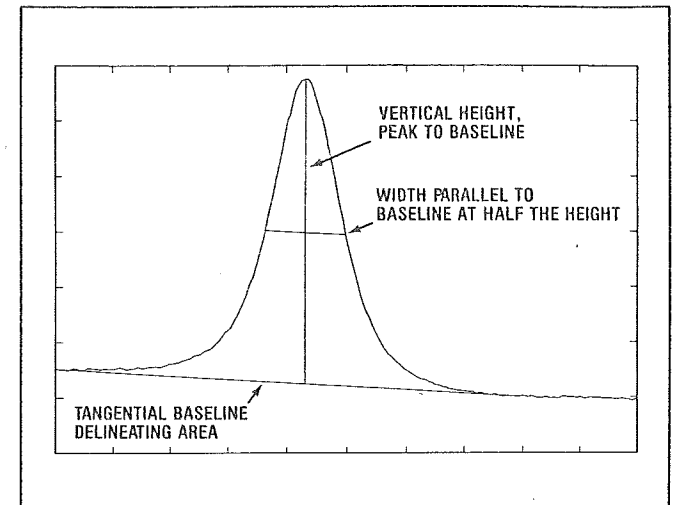


Figure 13. Method for determining height, width, and area of a photoelectron peak.

For a sample that is homogeneous in the analysis volume, the number of photoelectrons per second in a specific spectral peak is given by:

$$I = n f \sigma \theta y \lambda A T \quad (5)$$

where n is the number of atoms of the element per cm^3 of sample, f is the x-ray flux in photons/ $\text{cm}^2\text{-sec}$, σ is the photoelectric cross-section for the atomic orbital of interest in cm^2 , θ is an angular efficiency factor for the instrumental arrangement based on the angle between the photon path and detected electron, y is the efficiency in the photoelectric process for formation of photoelectrons of the normal photoelectron energy, λ is the mean free path of the photoelectrons in the sample, A is the area of the sample from which photoelectrons are detected, and T is the detection efficiency for electrons emitted from the sample. From (5):

$$n = I / f \sigma \theta y \lambda A T \quad (6)$$

$$\frac{I_1}{I_2} = \frac{n_1}{n_2} \cdot \frac{\sigma_1}{\sigma_2} \cdot \frac{\theta_1}{\theta_2} \cdot \frac{y_1}{y_2} \cdot \frac{\lambda_1}{\lambda_2} \cdot \frac{T_1}{T_2}$$

$$I T \lambda \propto E^{1.75}$$

The denominator in equation 6 can be assigned the symbol S , defined as the atomic sensitivity factor. If we consider a strong line from each of two elements, then:

$$\frac{n_1}{n_2} = \frac{I_1/S_1}{I_2/S_2} \quad (7)$$

This expression may be used for all homogeneous samples if the ratio S_1/S_2 is matrix independent for all materials. It is certainly true that such quantities as σ and λ vary somewhat from material to material (especially λ), but the ratio of each of the two quantities σ_1/σ_2 and λ_1/λ_2 , remains nearly constant. Thus, for any spectrometer, we may develop a set of relative values of S for all of the elements.

A generalized expression for determination of the atom fraction of any constituent in a sample, C_x , can be written as an extension of equation 7:

$$C_x = \frac{n_x}{\sum_i n_i} = \frac{I_x/S_x}{\sum_i I_i/S_i} \quad (8)$$

Values of S based on peak area measurements are indicated in Table 5 of the Appendix. These values are presented relative to the F1s intensity, which has been used as a standard. The values of S in the Appendix are based upon calculated values of σ^a which have been corrected for the kinetic energy dependence of the spectrometer detection efficiency and an average value for the dependence of λ on kinetic energy of $E^{0.75}$ (Figure 3). The values in the Appendix are only valid for, and should only be applied, when the electron energy analyzer used has the transmission

a) J. H. Scofield, J. Elect. Spectr. 8, 129 (1976).

characteristics of the double pass cylindrical-mirror type analyzer supplied by Physical Electronics. An example of the application of equation 8 to analysis of a nearly ideal sample, polytetrafluoroethylene, is shown in Figure 14.

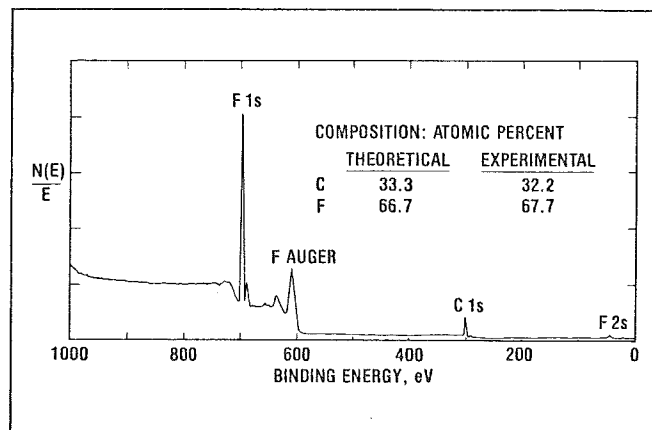


Figure 14. Quantitative analysis of polytetrafluoroethylene (by peak area of F1s and C1s).

The use of atomic sensitivity factors in the manner described will normally furnish semiquantitative results (within 10-20%) except in the following situations.

(1) The technique cannot be applied rigorously to heterogeneous samples. It can be useful with heterogeneous samples in obtaining results in terms of the relative number of atoms detected, but one must be conscious that the microscopic character of the heterogeneous system influences the quantitative results. Moreover, an overlying contamination layer has the effect of diminishing high binding energy peaks more than those with low binding energies.

(2) Transition metals, especially of the first series, have widely varying and low values of y , whereas y for the other elements is rather

uniform at about 0.8. Thus, a value of S determined on one chemical state for a transition metal may not be valid for another chemical state.

(3) When peak interferences occur, alternative lines must sometimes be used. The ratios of spin doublets (except 4p) are rather uniform and the weaker of the pair can often be substituted. Figure 15 is a general guide to the relative peak height of the minor lines. However, with the minor lines, there is much variation in relative peak heights and widths, so the figure should be regarded as a semi-quantitative guide, of the order of $\pm 30\%$. The sample spectra of the elements may also be consulted, but caution must be exercised, since the spectra of the elements themselves can be somewhat different, quantitatively, from the spectra of their compounds.

Occasionally an x-ray satellite from an intense photoelectron line interferes with measurement of a weak component. A mathematical approach can then be used to subtract the x-ray satellite before the measurement.

For quantitative work it is advisable to check the spectrometer operation frequently to ensure that analyzer response is constant and optimum. A useful test is the recording of the three widely-spaced spectral lines from copper. Measurement of peak height in counts per second should be made on 20 volt wide scans of the $2p_{3/2}$, LMM Auger, and 3p lines, and the peak width of the $2p_{3/2}$ line should be measured as shown in Figure 13. Maintenance of such records makes it easily noticeable if an instrumental change occurs that would affect quantitative analysis.

E. DETERMINATION OF ELEMENT LOCATION

(1) Depth. There are four methods of obtaining information on the depth of an element in the sample. The first two methods below utilize the characteristics of the spectrum itself, but provide limited information. The third, depth profiling by erosion of the surface, provides more detailed information but is attended by certain problems. The fourth utilizes measurements at two or more electron escape angles.

i. The presence or absence of an energy loss peak or envelope indicates whether the emitting atoms are in the bulk or at the surface. Since electrons from surface atoms do not traverse the bulk, peaks due to the surface atoms are symmetrical above level baselines on both sides and the energy loss peak is absent.

ii. Elements whose spectra exhibit photoelectron lines widely spaced in kinetic energy can be approximately located by noting the intensity ratio of the lines. In the energy range above approximately 100 eV, electrons moving through a solid with lower kinetic energy are attenuated more strongly than those with higher kinetic energy. Thus, for a surface species, the low kinetic energy component will be relatively stronger than the high kinetic energy component, compared to that observed in the pure material. The data in Figure 15 for homogeneous bulk solids can be compared with intensity ratios observed on unknowns to determine qualitatively the distribution of the element in the sample. Suitable elements include Na and Mg (1s and 2s); Zn, Ga, Ge, and As ($2p_{3/2}$ and 3d); and Cd, In, Sn, Sb, Te, I, Cs, and Ba ($3p_{3/2}$ and 4d, or $3d_{5/2}$ and 4d).

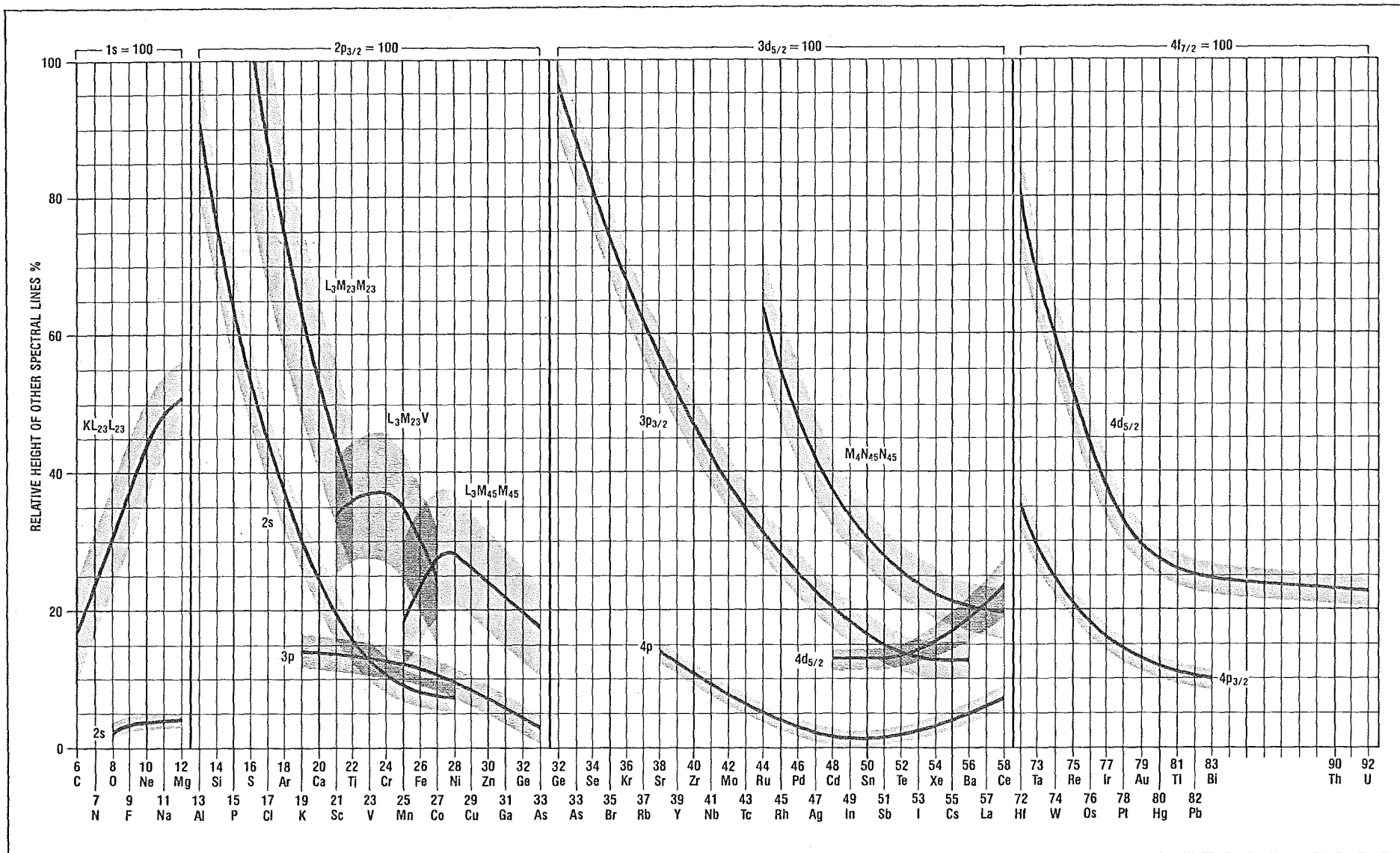


Figure 15. Peak heights of minor lines relative to strong lines (based on survey spectra contained herein).

For the situation where the element is in a bulk homogeneous layer beneath a thin contaminating layer the characteristic intensity ratio is modified in the opposite direction. Thus, for a pair of lines due to subsurface species, the low kinetic energy line will be attenuated more than the high kinetic energy line, distorting the characteristic intensity ratio. By observing such intensity ratios and comparing them with the values for pure bulk elements (Figure 15), it is possible to deduce whether the observed lines are due to predominantly surface, subsurface, or homogeneously distributed material.

iii. Depth profiling can be accomplished by controlled erosion of the surface by ion sputtering. In Table 4 are presented some data on sputter rates as a general guide. One can use this technique on organic materials, but few data are available for calibration. Chemical states are usually changed by the sputter technique, but useful information on elemental distribution still can be obtained.

Table 4 — Some representative sputter rates

(2 keV argon ion beam with 100 μ amps/cm² impinging on sample)

Target	Sputter Rate, Å/min ^{a)}
Ta ₂ O ₅	100
Si	90
SiO ₂	85
Pt	220
Cr	140
Al	95
Au	410

a) \pm 20%.

Another method of controlled erosion that is useful, especially with organic materials, is reaction with oxygen atoms from a plasma. This technique may also change the chemical states in the affected surface. Further, since the elements differ in their rates of reaction with oxygen atoms, the rate of removal of surface materials will be somewhat sample dependent.

iv. One may alter the angle between the plane of the sample surface and the angle of entrance to the analyzer. At 90°, with respect to the surface plane, the signal from the bulk is maximized relative to that from the surface layer. At small angles, the signal from the surface becomes greatly enhanced, relative to that from the bulk. The location of an element can thus be deduced by noting how the magnitude of its spectral peaks change with sample orientation in relation to those from other elements.

The electron energy analyzer used in the ESCA/SAM incorporates a special aperture arrangement that permits angular resolved studies. An example of the information that can be gained through the use of this capability is shown in Figure 16. Data were obtained at high (near 90°) and low (near 15°) exit angles from a silicon sample with a thin silicon oxide overlayer. The observed intensity ratio of oxidized to elemental silicon is much greater at the small exit angle.

(2) Insulating Domains on a Conductor. The occurrence of steady-state charging of an insulator during analysis sometimes has useful consequences. Microscopic insulating domains on a conductor reach their own steady-

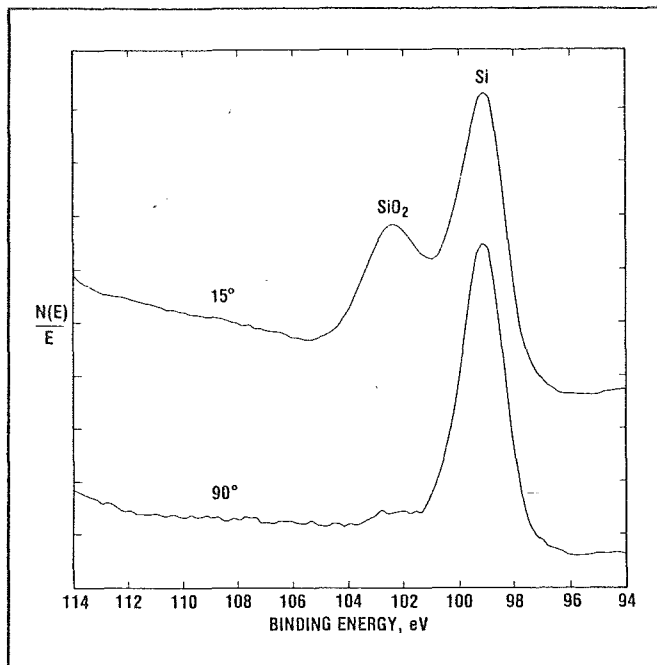


Figure 16. Use of different electron escape angles to determine depth distribution (Si 2p line from silicon sample with approximately one monolayer SiO₂ overlayer). Angles indicated are electron take-off angles relative to specimen surface.

state charge, while the conductor remains at spectrometer potential. Thus, an element in the same chemical state in both phases will exhibit two peaks. If a change is made in the supply of low energy electrons which stabilize the charge, as from the neutralizer filament, or if a bias is applied to the conductor, the spectral peaks from the insulating phase will move relative to those from the conducting phase, as shown in Figure 17. For such heterogeneous systems, this is an extremely useful technique. It makes it possible to determine whether the elements that contribute to the overall spectrum are in the conducting or the insulating phase, or in both phases.

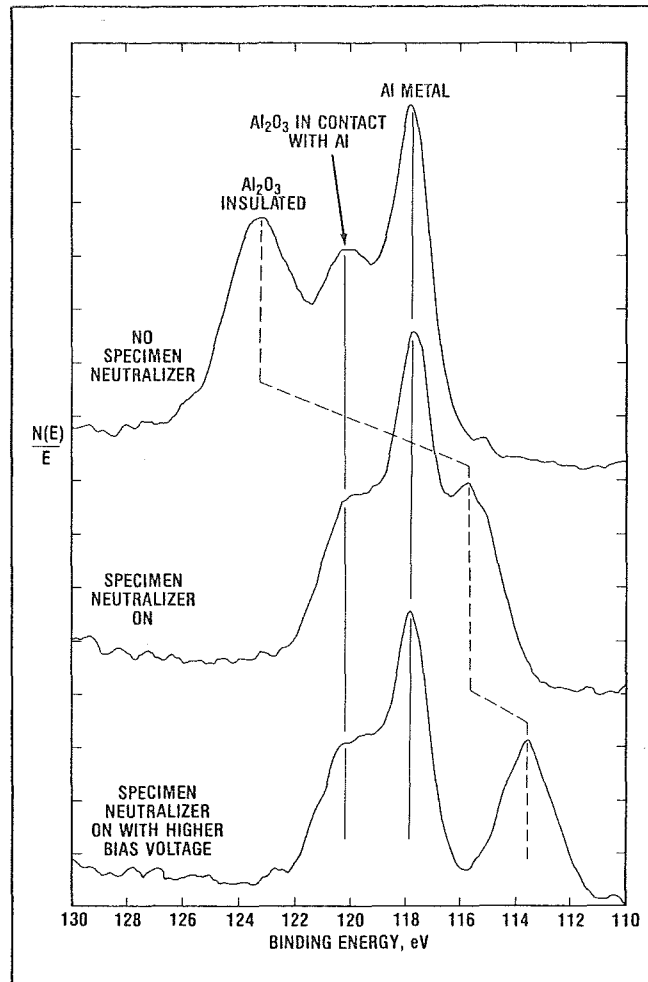


Figure 17. Use of specimen neutralizer to shift the partial spectrum from insulating domains (Al 2s lines from Al₂O₃ on aluminum sample).

(3) Surface Distribution. ESCA is not ordinarily used to obtain information on X-Y distribution because a large analysis area is required for good signal intensity. With the PHI double pass cylindrical-mirror analyzer used in the ESCA/SAM, however, a circular area of 2-5 mm diameter can be imaged, depending upon the apertures in use and the retarding condi-

tions. This area is expressed as the full width at half maximum of the photoelectron intensity observed as a function of distance from the center of the imaged area. Thus, the effective

sample area is not large. It is often possible to analyze different positions on the same sample when the surface is heterogeneous on a scale larger than two millimeters.

6. How to Use This Handbook

Full utilization of this Handbook can best be accomplished by following these procedures.

A. FOR QUALITATIVE ANALYSIS

The elemental and chemical identification of sample constituents can be performed most readily by combining the information in the standard survey spectra in Section II with the binding energy tables (Tables 1-4) presented in the Appendix.

- (1) First identify all major photoelectron peaks utilizing the line position tables (Tables 1-4, pages 182-187).
- (2) Check to see that the determinations made in step 1 are consistent with the standard survey spectra.
- (3) Identify the Auger electron peaks by the line positions listed in Tables 1-4 in the Appendix (these are different for Mg and Al x-ray sources) and the expanded spectra provided for many of the elements in Section II.
- (4) Review section I.5.A. (p. 12) to account for fine structure such as energy loss lines, shake-up peaks, satellite lines, etc. not identified in Handbook spectra or energy tables.

(5) Identify any remaining small peaks, assuming they are intense photoelectron or Auger lines of minor constituents using Tables 3 and 4.

(6) Chemical state identification can be deduced from high energy resolution ($E_{\text{pass}} \leq 25 \text{ eV}$) spectra of the strongest photoelectron lines and sharpest Auger lines.

i. Review Section I.5.C. (p. 17) to correct binding energies for static charging of insulators. When applicable, charge reference the binding energy scale to the hydrocarbon C1s photoelectron peak (BE = 284.6 eV).

ii. Use the tabulated experimental data and standard high energy resolution spectra to determine the chemical state from measured shifts in the photoelectron binding energies (cf section I.5.C., p. 18).

iii. For the elements F, Na, Cu, Zn, As, Cd, In, and Te, convert corrected Auger line positions to kinetic energies by subtracting from the photon energy (Mg = 1253.6, Al = 1486.6 eV). Note the location of the points for Auger kinetic energy and photoelectron binding energy on the respective elemental plot. Proximity of experimental points to

those of recorded chemical states should be considered probable identification, if consistent with other elemental findings and with calculated stoichiometry (see below). Note that experimental error in point location is much greater along the Auger parameter grid than normal to the grid lines.

iv. As suggested in the text (Section I.5.C., p. 20), much can be determined about the chemical state from the magnitude and position of shake-up lines as well as the energy and shape of valence Auger electron lines.

B. FOR QUANTITATIVE ANALYSIS

The atomic sensitivity factors (S_x) presented in Table 5 of the Appendix (p. 188) were calculated according to theoretical photoelectron cross sections, the kinetic energy dependence of the PHI Precision Electron Energy Analyzer and an average value for the dependence of the electron escape depth on kinetic energy. A simplified expression to determine the atomic

concentration (C_x) of any element x is given in equation 8:

$$C_x = \frac{I_x/S_x}{\sum_i I_i/S_i} \quad (9)$$

where I_x is the relative peak area of photoelectrons from element x . However, it must be pointed out that the method is limited in accuracy by the assumptions made (cf Section I.5.D., p. 21).

The spectrum should be examined with a view to finding information on the depth of the element (i.e., by peak intensity ratios, or the presence or absence of loss lines). Further scans with variable take-off angle, or by erosion of the surface, can be made if this point needs further elucidation.

C. FOR A FINAL CHECK

A concluding effort should be made to ensure that quantitative data and the conclusions on chemical state are consistent. This includes quantitative apportionment of an element among two or more chemical states, where that is indicated.

II. STANDARD ESCA SPECTRA OF THE ELEMENTS AND LINE ENERGY INFORMATION

This section of the Handbook contains survey (broad scan) spectra of sixty-eight elements, detail spectra of the strongest photoelectron lines, and a photoelectron binding energy chart or a two-dimensional Auger parameter plot for each of the sixty-eight elements. Used in combination with the Tables in the Appendix, the survey spectra facilitate element identification. The detail spectra and charts aid in the identification of chemical states.

SURVEY SPECTRA

The broad scans include all of the lines that are normally useful. The photoelectron and more prominent Auger lines for the element of interest are identified. Lines that occur due to other elements are only designated by the elemental symbol, and x-ray satellites and energy loss lines are not noted. Many elements exhibit x-ray generated Auger lines which have sufficient sharpness and structure to be useful. For these elements, the Auger region is displayed in expanded form. Exact energies of the sharper Auger lines are noted. The energies of those that are less sharp are recorded to the nearest electron volt. The instrumental contribution to the line width is 1.0 eV (50 volts pass energy) for the broad scans.

The Y scale has been left undesignated because it was not possible to control the surface roughness of the standards. However, the general contours and relative intensity ratios in the spectra should be typical of measurements made with the PHI Precision Electron Energy Analyzer in the retard mode.

DETAIL SPECTRA

The detail spectra of the strongest photoelectron lines are presented opposite the survey spectra. In all cases, the binding energy of the main line is in-

dicated and, where appropriate, the spin doublet separation is noted. When necessary, checks were made to ensure that chemical states were unchanged by the radiation. The lines from insulators have been charge-corrected to the adventitious hydrocarbon C1s line at 284.6 eV. The instrument was, in all cases, calibrated to place the Au4f_{7/2} line at 83.8, Cu3p_{3/2} line at 74.9, and the Cu2p_{3/2} line at 932.4 eV. The instrumental contribution to the line width for the detail spectra is 0.5 eV (25 volts pass energy).

PHOTOELECTRON BINDING ENERGY AND TWO-DIMENSIONAL AUGER PARAMETER CHARTS

The photoelectron binding energy charts have been constructed utilizing data available in the literature up to 1978. Data from the experimental work contained in this section have been included and denoted by the symbol Φ . Data from literature references have not been included if the method of charge referencing is unknown or of questionable validity. Data included are all referred to a binding energy scale with Au4f_{7/2} = 83.8 and C1s = 284.6 eV, although it is recognized at this time that general agreement has not been reached and that the values 84.0 and 284.8 could have been chosen with equal justification. It is likely that the values ultimately agreed upon will be within these limits.

Line positions have been shown as bars 0.2 eV wide, although with insulating materials the error may be somewhat larger. Data available for C, N, O, P, S, Cl, K, Cr, Mn, Fe, Co, Ni, Mo, Rh, Pd, Sn and Pt were numerous, and selection was made of those chemical states deemed most useful. Multiple data on the same chemical state are frequently included to indicate reproducibility in different laboratories. Data that are obviously outlying have been rejected, but where some doubt existed on the selection, disagreeing values were included.

Two-dimensional chemical state plots accompany the spectra for F, Na, Cu, Zn, As, Ag, Cd, In and Te. In the format adopted, the kinetic energy of the Auger line is plotted against the binding energy of the photoelectron line, with the latter plotted in the $-x$ direction (kinetic energy is still, implicitly, $+x$). The points on the two-dimensional plot are drawn as rectangular boxes at 45° , reflecting the expected error of measurement in the two perpendicular directions.

References for the one and two-dimensional plots were catalogued by initials of the first three authors. Where two or more identical symbols for references would have resulted, a final differentiating number was added. The entire reference list is presented in Section II-2 (p. 174). Those in the list

that are marked with an asterisk have many more data besides those listed here.

Abbreviations used in the tables and plots include the following:

R	= alkyl	acac	= acetylacetonate
Me	= methyl	ox	= surface oxidized in air
Et	= ethyl	sulf	= surface treated with H_2S
Pr	= propyl	p-	= para
Bu	= butyl	aq	= hydrate
Am	= amyl	tu	= thiourea
Ph	= phenyl	tm	= tetramethylthiourea
Ac	= acetyl	cp	= cyclopentadiene
Bz	= benzyl		
bae	= ethylenediamine + acetylacetonate (condensation product)		
salen	= ethylenediamine + 2 salicylaldehyde (condensation product)		